Atmos. Chem. Phys. Discuss., 6, 9431–9458, 2006
www.atmos-chem-phys-discuss.net/6/9431/2006/

Atmospheric Chemistry and Physics Discussions

High resolution vertical distributions of NO_3 and N_2O_5 through the nocturnal boundary layer

S. S. Brown[1], **W. P. Dubé**[1,2], **H. D. Osthoff**[1,2], **D. E. Wolfe**[1], **W. M. Angevine**[1,2], and **A. R. Ravishankara**[1,3]

[1]NOAA Earth System Research Laboratory, 325 Broadway, Boulder, CO 80305, USA
[2]Cooperative Institute for Research in Environmental Science, University of Colorado, Boulder, CO 80305, USA
[3]Department of Chemistry and Biochemistry, University of Colorado, Boulder, CO 80309, USA

Received: 30 August 2006 – Accepted: 12 September 2006 – Published: 26 September 2006

Correspondence to: S. S. Brown (steven.s.brown@noaa.gov)

Abstract

The shallow mixing depth and vertical stratification of the lowest levels of the atmosphere at night has implications for the chemistry of nitrogen oxides emitted from the surface. Here we report vertical profiles of NO_3, N_2O_5 and O_3 measured from in-situ instruments on a movable carriage on a 300 m tower. The study offers high-resolution (<1 m) vertical distributions of both NO_3 and N_2O_5 and shows that the nocturnal mixing ratios of these compounds vary widely over short vertical distance scales (10 m or less). Furthermore, there are systematic differences in the steady state lifetimes of NO_3 and N_2O_5 and in the partitioning among nitrogen oxides between different near-surface layers. These differences imply that NO_3 and N_2O_5 occupy distinct chemical regimes as a function of altitude, potentially serving as sinks for nitrogen oxides and O_3 near the surface but as reservoirs of NO_x and O_3 aloft.

1 Introduction

Atmospheric nitrogen oxide chemistry near the Earth's surface is strongly linked to the dynamics of the planetary boundary layer. During the day, the typical depth of a summertime convective boundary layer is on the order of 1.5 km, although the depth and the efficiency of mixing can be influenced by a number of factors (Stull, 1988). Daytime surface emission of NO_x (= the sum of NO and NO_2, but emitted mainly as NO) are mixed to the boundary layer depth and enter into the well-known catalytic cycle that generates photochemical ozone pollution (Chameides, 1978). By contrast, the nocturnal boundary layer has a depth of order 0.1 km and is less efficiently mixed. As a result, nocturnal NO_x emissions tend to be more concentrated and vertically stratified than daytime emissions. The stratification is coupled to a shift in nitrogen oxide chemistry; at night, NO_x oxidizes in the presence of excess ozone to the nocturnal nitrogen oxides, NO_3 (the nitrate radical) and N_2O_5 (dinitrogen pentoxide), which may serve either as reactive intermediates that convert NO_x to nitric acid and other prod-

ucts (Richards, 1983) or as nocturnal reservoirs of NO_x and O_3 (Brown et al., 2006). Because both the sources and the sinks for NO_3 and N_2O_5 can be spatially stratified, their mixing ratios, and their influence on nitrogen oxide and ozone transport and loss at night can show large variability as a function of height above the surface.

Because of this nocturnal atmospheric chemical – dynamical coupling, the vertical distribution of nitrogen oxide species at night, particularly NO_3, has been a topic of considerable recent interest. Modeling studies have consistently suggested strong vertical gradients of NO_3 and N_2O_5 within the nocturnal boundary layer (Fish et al., 1999; Galmarini et al., 1997; Geyer and Stutz, 2004a, b; Riemer et al., 2003). Experimental studies with sufficient resolution to confirm these predictions have been sparse, however. Vertical profiles of NO_3 in the troposphere have been retrieved from the time dependence of the NO_3 absorption spectrum in a slant column of scattered sunlight at sunrise, as solar photolysis removes NO_3 radicals to progressively lower altitudes (Aliwell and Jones, 1998; Allan et al., 2002; Coe et al., 2002; Saiz-Lopez et al., 2006; Smith and Solomon, 1990; Smith et al., 1993; von Friedeburg et al., 2002; Weaver et al., 1996) Aside from the work of von Friedeberg et al. (2002) this method has typically had insufficient resolution to determine profiles within the boundary layer, although it has commonly been used to determine total boundary layer column absorptions. Broadband lidar measurements have also been used to measure the total column abundance of NO_3 within the boundary layer (Povey et al., 1998). Both of these approaches have shown average boundary layer concentrations of several hundred pptv of NO_3, well in excess of typical surface-level NO_3 mixing ratios. Stutz and coworkers (Stutz et al., 2004; Wang et al., 2006) have more recently achieved a resolution of several tens of meters within the boundary layer for continuous measurements of NO_3, NO_2, O_3 and other trace gases throughout the night via multiple long path differential optical absorption spectrometers (DOAS) aligned over several fixed slant paths between 0–140 m. These measurements have shown significant gradients in NO_3 within the nocturnal boundary layer.

This paper presents results from a preliminary study of the vertical distribution of the

nocturnal nitrogen oxides, NO_3 and N_2O_5, at high spatial resolution (<1 m) within and above the nocturnal boundary layer. Mixing ratios of both NO_3 and N_2O_5 were measured in-situ from an instrument mounted on a movable carriage on a 300 m tower. Although this study is rather limited in scope, encompassing only a single night in October, 2004 with a limited set of ancillary data, it is unique both because of its high vertical resolution and because of the direct measurement of N_2O_5 vertical profiles. The ability to independently measure N_2O_5 can be important, not only because of its much larger mixing ratio relative to NO_3 in high NO_x and/or cold environments, but also because of its non-linear dependence on NO_2, which can make its calculation from column measurements of NO_3 and NO_2 under conditions of high spatial variability potentially problematic. The study shows that NO_3, N_2O_5, NO_2 and O_3 are quite variable over short distance scales within the nocturnal boundary layer and that there are systematic and often sharp changes at the interface between the nocturnal boundary layer and the residual, daytime boundary layer above it. The results are broadly consistent with the expected behavior of NO_3 and N_2O_5 from previous experimental and theoretical studies, but show that the detailed vertical profiles of these compounds, at least at this measurement site, can be quite complex.

2 Experimental

The measurements took place at the Boulder Atmospheric Observatory (BAO) (Hahn, 1981; Kaimal and Gaynor, 1983; Vanvalin and Ganor, 1987) located in Erie, CO, USA on the night of 4–5 October 2004. Figure 1 is a map of the Boulder / Denver area showing the location of the observatory in relation to these cities (Boulder 25 km to the West, Denver 35 km to the South). The site is in an area of mixed rural/suburban development and is impacted by anthropogenic emissions from the broad urban and suburban area of Colorado's front range cities. The area immediately surrounding the observatory is grassland, and the closest large local emission sources include a landfill 3 km to the Southwest and a major highway (Interstate 25) 2 km to the East. The city

of Erie, with its accompanying recent suburban development, is 3.5 km to the West.

The tower itself is 300 m in height, with its base at 1584 m above sea level. It has a motorized external carriage that can ascend or descend the tower at a rate of ~0.6 m s^{-1}. The carriage can also be positioned indefinitely at an arbitrary height. The drive on the carriage is electric and does not produce emissions that we are aware of or that were detectable by the instruments during this study. There are meteorological stations at fixed heights of 10, 50, 100, 200 and 300 m, although not all of them were working properly at the time of this study.

In-situ measurements of NO_3 and N_2O_5 were carried out using a instrument based on cavity ring-down spectroscopy that had been designed for deployment on the NOAA P-3 aircraft (Dubé et al., 2006). This instrument had a time resolution of 1 s (vertical resolution of 0.6 m for this study), detection sensitivity of 0.4–2 pptv, and an accuracy of 25%, limited mainly by uncertainties in the inlet transmission efficiency of the two compounds. The instrument measures NO_3 by direct absorption at 662 nm (pulsed dye laser) in an ambient channel, and the sum of NO_3 and N_2O_5 simultaneously in a second, heated channel using the same light source. The instrument was mounted directly to the carriage, with the air sample introduced through a 40 cm length of PFA Teflon tubing. Mixing ratios of O_3 were measured at lower time resolution (18 s) from the same inlet using a commercial O_3 monitor (total uncertainty = 2%±2 pbbv). A thermocouple probe located at the tip of the inlet provided a continuous ambient temperature measurement. The mixing ratio of NO_2 was not measured, but may be calculated from the ratio of N_2O_5 to NO_3 and the ambient temperature.

$$[NO_2]_{calc} = \frac{[N_2O_5]}{K_{eq}(T) \times [NO_3]} \quad (1)$$

Here $K_{eq}(T)$ is the temperature-dependent equilibrium constant for the reversible association of NO_2 with NO_3 to form N_2O_5, taken from the NASA/JPL recommendation (Sander et al., 2003). Previous field studies of this equilibrium in which all three components (i.e., NO_2, NO_3 and N_2O_5) were measured showed it to be in agreement with

the calculated equilibrium to within 30% (Brown et al., 2003b); therefore, this is a reasonable estimate for the uncertainty of the calculated NO_2, with the exception of data for which the mixing ratio of NO_3 was small; no calculated NO_2 data are reported for an arbitrary threshold of NO_3 smaller than 3 pptv.

3 Results

The measurement period was from 16:40 on 4 October, or approximately 2 hours prior to local sunset, to 08:10 on 5 October, approximately 1 h after local sunrise. Figure 2 shows a time series of the measured mixing ratios of NO_3, N_2O_5 and O_3, as well as the sample altitude. Peak mixing ratios of NO_3 and N_2O_5 were 90 pptv and 2 ppbv, respectively, but were uniformly smaller during periods when the carriage was at the bottom of the tower. Mixing ratios were larger earlier in the night under southerly flow than early in the morning, when the flow shifted to westerly. The available meteorological data at different, fixed heights appears in Fig. 3. There were a total of 37 individual vertical profiles (8–9 min each) that spanned the entire 300 m range of the tower and multiple shorter profiles spanning smaller ranges. Of the 37, 300 m profiles, 27 were during darkness (between sunrise and sunset). Figure 4 shows 30 of the profiles taken from just prior to sunset until just after sunrise. There was considerable variability in both the overall concentrations of NO_3 and N_2O_5 between different profiles and in their distribution within individual profiles as a function of altitude. Variations between profiles were in some cases clearly evident even on vertical profiles taken only a few minutes apart. Nevertheless, many of the profiles fell into reasonably distinct categories with similar characteristics. The primary criterion for categorizing profiles was the vertical variation in potential temperature, Θ, taken as a measure of the small-scale stratification and layering.

The observations frequently showed a three-layer structure, as shown in more detail Fig. 5. For purposes of this paper, we will use the following terms: the strongly stable layer extending from the surface to ~20 m will be called the surface layer. The statically

stable layer above this, up to 100–150 m, is the nocturnal boundary layer (NBL). Atop this layer, we commonly observed an increase of stability over 10–20 m, which we will refer to as the top of the nocturnal boundary layer. Although this could be considered a separate layer, the chemical observations (see below) indicated that this structure functioned as an interface. The uppermost layer, above ~150 m, is called the residual layer (i.e., the remnant of the deeper, well-mixed daytime boundary layer). In using this term, we presume that this layer had not been strongly affected by the surface since the previous afternoon.

Each of the sections below contains a discussion of an example profile, and the last section discusses a composite profile made up of several individual profiles. The discussion here is largely qualitative; the limited set of measurements available for this pilot study does not allow for detailed analysis or modeling of the chemical sinks for NO_3 and N_2O_5 or their variation with altitude.

3.1 Example 1: three layer profile

An example of a three layer profile, taken during SSW flow between 23:15–23:23, is shown in Fig. 6. The chemical measurements within this particular profile exhibited a smooth variation within each layer that correlated with the temperature variation in a well-defined manner. The left hand graph shows the vertical profile of the NO_3 and N_2O_5 mixing ratios and the potential temperature, Θ (top axis). The potential temperature profile and layering is the same as that shown in Fig. 5, with a stable surface layer extending to 10–20 m and an NBL extending to 120 m. The mixing ratio of N_2O_5 decreased rapidly toward the ground within the surface layer, consistent with a sink for NO_3 and N_2O_5 at the ground surface (see discussion below). Within the NBL, N_2O_5 concentrations peaked and then declined with increasing height, while NO_3 was relatively constant or slightly increasing. These changes imply a vertical gradient of decreasing NO_2, whose calculated values are shown in the center graph of Fig. 6. The vertical profiles in NO_3, N_2O_5 and calculated NO_2 were also consistent with the observed increase in O_3 with height within this layer, also shown in the center graph of

Fig. 6. A decrease in NO_2 shifts the equilibrium between NO_3 and N_2O_5 in favor of NO_3 while at the same time decreasing the production rate for NO_3 from the reaction of NO_2 with O_3 (i.e., $k_2[O_3][NO_2]$ from reaction 2, below). By contrast, the increasing O_3 concentration increases the source strength with height.

$$NO_2 + O_3 \rightarrow NO_3 + O_2 \qquad k_2(286\,K) = 2.3 \times 10^{-17} cm^3\,s^{-1} \tag{2}$$

The rate coefficient (Sander et al., 2003) is given for the average temperature during darkness on 4–5 October. The inverse relationship between O_3 and NO_2 through the NBL is consistent with emission of NO_x near the surface and consequent titration of O_3 by reaction with NO.

$$NO + O_3 \rightarrow NO_2 + O_2 \qquad k_3(286\,K) = 1.6 \times 10^{-14}\,cm^3\,s^{-1} \tag{3}$$

The net increase in NO_2 toward the surface was approximately equal to the net decrease in O_3, implying that the mixing through the NBL is slow enough relative to the rate of NO_x emission to maintain a vertical gradient. Wang et al. (2006) have noted similar behavior in NO_2 and O_3 within the NBL.

The vertical gradients in the reactivity of NO_3 and N_2O_5 and the partitioning between the nitrogen oxide species can be seen in the right hand panel of Fig. 6. The steady state lifetimes of NO_3 and N_2O_5 are the ratios of their observed concentrations to their source strength (Brown et al., 2003a; Heintz et al., 1996; Platt et al., 1984).

$$\tau(NO_3) = \frac{[NO_3]}{k_2[NO_2][O_3]}; \quad \tau(N_2O_5) = \frac{[N_2O_5]}{k_2[NO_2][O_3]} \tag{4}$$

Under conditions where NO_3 and N_2O_5 achieve an approximate steady state between their source and their loss due to reactions of NO_3 with NO or VOC and/or heterogeneous hydrolysis of N_2O_5, these lifetimes are a measure of the reactivity of the sum of the two compounds. (Note that the lifetimes are not separable; sinks for NO_3 influence the lifetime of N_2O_5 and vice versa.) On this night, the time required for the NO_2-NO_3-N_2O_5 system to achieve steady state would have been slow (several hours or more)

because of the relatively cool temperatures and the large amount of NO_2 near the surface (Brown et al., 2003a). Furthermore, Geyer and Stutz (Geyer et al., 2004a) have argued that vertical transport and mixing of N_2O_5 in the presence of strong vertical gradients can also limit the applicability of steady-state lifetimes. The observed steady state lifetimes were therefore only approximate measures of NO_3 and N_2O_5 sinks, and were most likely a lower limit to the values that would have been achieved at longer times.

Qualitatively at least, the relative changes in lifetime with height in Fig. 6 are an indication that there was a distinct shift between two regimes in NO_3 and N_2O_5 reactivity occurring at the top of the NBL, with much shorter steady state lifetimes within the NBL than in the residual layer. The change occurred over a distance scale of only a few tens of meters. Lifetimes above the boundary layer were as long as 3 h for N_2O_5, and even this was likely a lower limit (see above). The much smaller lifetimes within the boundary layer were consistent with the co-emission of NO_3 and N_2O_5 sinks with the NO_x that was their source. For example, reactive VOC and aerosol emitted from surface sources are likely to be trapped below the nocturnal inversion. Based on the NO_3 and N_2O_5 lifetimes alone, it is not possible to determine which of the two possible loss pathways contributes more to the reactivity of the pair within the boundary layer. Potential loss processes for both are discussed further in Sect. 4.

The partitioning, $F(NO_x)$, among the nitrogen oxides is a measure of the proportion of nitrogen oxide stored in the nocturnal reservoir of NO_3 and N_2O_5 (Brown et al., 2003b).

$$F(NO_x) = \frac{NO_3 + 2 \times N_2O_5}{NO_2 + NO_3 + 2 \times N_2O_5} \quad (5)$$

The variation of $F(NO_x)$ with height in Fig. 6 (right hand graph, top axis) is consistent with the trends in lifetime in the same graph. Within the NBL, where the lifetimes suggest rapid sinks for NO_3 and N_2O_5, the partitioning was less than 10%, but increased steadily with height. Similar to the observed trend in lifetimes, a step increase occurred at the top of the NBL, with partitioning levels above reaching 35%. Under the

assumption that there was no mixing of NO_x emission from the surface to the residual layer after sunset, numerical integration of NO_3 and N_2O_5 formation at 50 ppbv of O_3 indicates a maximum value for $F(NO_x)$ (i.e., no loss of NO_3 or N_2O_5) of approximately 55%. The observed value of 35% shows that NO_3 and N_2O_5 aloft acted primarily as a reservoir for NO_x, and could be expected to store or transport a large fraction of the available NO_x until sunrise. Within the boundary layer, the opposite was true; the apparently faster reactivity of NO_3 and N_2O_5 inferred from the lifetimes, and the slower oxidation of NO_2 by the reduced O_3 level prevented storage of a significant fraction of NO_2 in the nocturnal nitrogen oxide reservoir. Within this layer, NO_3 and N_2O_5 appear to have served as sinks, rather than reservoirs, for NO_x.

3.2 Example 2: two layer profile

Although the surface layer was a common feature in many of the temperature profiles, it was absent in 6 of 12 profiles taken late in the night, between 02:30 and sunrise. In these profiles, the NBL extended continuously down to the lowest measurement height (3 m above ground). Figure 7 shows an example of one such profile, taken between 03:06–03:14. The only clear feature in the temperature profile was a layer of greater stability at 165 m, taken as the top of the NBL. Mixing ratios of NO_3 and N_2O_5 were somewhat variable within this layer, but were not clearly systematic with height. Within the residual layer, by contrast, both increased systematically with height. Profiles of calculated NO_2 and measured O_3 were similar to those seen in Fig. 6, showing increasing NO_2 and decreasing O_3 toward the surface within the NBL. The total amount of NO_x was smaller in this profile, consistent with a wind shift to the West and Northwest that took place later in the night. The trends in the steady state lifetimes and in partitioning in the right hand graph were similar to those in Fig. 6, with larger values in the residual layer than in the boundary layer. However, the transition between the two regimes was much less abrupt. Above the boundary layer, the increase in lifetimes and partitioning was continuous, with a maximum $\tau(N_2O_5)$ of 5 h (very likely a lower limit) and $F(NO_x)$ in excess of 40% at the maximum height of 300 m above

ground. The partitioning value is slightly more than half of the maximum possible (see preceding section), calculated in this case to have been 70–75%. The upward trend with height suggests that above the tower these values may have continued to increase.

3.3 Example 3: multiple layer profile

The profiles in Figs. 6–7 show relatively smoothly varying changes in temperature and chemical composition with height. There were also several profiles in which this was not the case, as shown by the example in Fig. 8. This profile, taken between 22:05–22:13, showed the same shallow surface layer seen in Fig. 6. In this case, however, there were at least two additional layers within the first 100 m above ground. The mixing ratio of N_2O_5 showed large spatial variability that correlated with the changes in the temperature profile. The N_2O_5 profile, and the NO_2 profile inferred from it, both indicate that there may have been additional layering correlated to some of the smaller features in the temperature profile (e.g., sharp spike near 140 m.) The O_3 profile was also more variable below approximately 150 m than in the preceding examples, although the time resolution of this measurement was not sufficient to capture fine-scale structures correlated with the variations in N_2O_5. The variable O_3 levels below 150 m and relatively constant O_3 levels above may indicate that this was the height to which surface emission had been recently mixed, even though the temperature profile did not show a clear stable layer at this point.

The lower time resolution of the O_3 measurement, and the lack of calculated NO_2 within the lowest part of the profile due to values of NO_3 below the detection limit (making the ratio of N_2O_5 to NO_3 unmeasurable), made it impossible to assess the correlation of the steady state lifetimes in the right hand graph with the temperature and chemical fluctuations seen in the other profiles. However, as with all of the preceding examples (and indeed, as with every profile for which lifetimes could be calculated), the lifetimes showed a clear increasing trend with height. Above 90 m in Fig. 8, the lifetimes appear to show a relatively smaller degree of layering and/or stratification than do the levels of NO_3, N_2O_5 and NO_2. This may imply that even though the NO_x occurred in

relatively discrete layers, the sinks for NO_3 and N_2O_5 varied more smoothly with height above the surface.

3.4 Profile averages

The averages of the 23 individual profiles recorded between 19:00 (23 min after sunset) and 06:00 (1 h prior to sunrise) appear in Figure 9. The two left hand graphs show the average measured NO_3, N_2O_5 and O_3 mixing ratios and the average potential temperature. Many of the trends discussed above for the individual profiles were also apparent in the averages. The surface layer was a consistent feature and is evident as a sharp decrease in the average Θ in the lowest few tens of meters. The top of the NBL, on the other hand, was variable between 100–250 m in individual profiles. As a result, the averaged Θ showed a continuous increase with height above the surface layer without a characteristic discontinuity. A clearer measurement of the average depth of the NBL was evident at 150 m from the O_3 measurement. Below this level, average O_3 decreased continuously as a result, presumably, of surface emissions of NO_x and surface deposition of O_3. Average mixing ratios of NO_3 and N_2O_5 showed a smoothly-varying, continuous increase from the ground up with no obvious signature of the NBL.

The right hand graph of Fig. 9 shows the relative standard deviation (i.e., the quotient of the standard deviation and the average within each 1 m increment from all profiles) in NO_3, N_2O_5 and O_3 with height. The variability in NO_3 and N_2O_5 was similar and was smaller aloft than at the surface, showing no trend with height above 150 meters but increasing steadily below 100 m. Within the surface layer, $\delta(NO_3)$ and $\delta(N_2O_5)$ increased sharply. The trend in O_3 variability was similar, except that $\delta(O_3)$ was consistently smaller and did not show a sharp increase within the surface layer (possibly as a result of the lower time resolution of the measurement). The larger variability in O_3, NO_3 and N_2O_5 within the NBL compared to above it may have been due to variations in a number of factors, including the amount of NO_x mixed into the boundary layer, the boundary layer depth or sinks for NO_3 and N_2O_5.

4 Discussion

The temperature profiles and the chemical composition measurements are consistent with reduced mixing, stratification and layering in the lowest few hundred meters of the atmosphere at night. Although the picture was sometimes more complicated, the vertical structures could generally be grouped into the three categories shown in Fig. 5. The layers were associated not only with changes in chemical composition (i.e., NO_x and O_3), but also with reactivity of the nocturnal nitrogen oxides, NO_3 and N_2O_5 as inferred from their steady state lifetimes and nitrogen oxide partitioning. Because of the lack of ancillary measurements, it is not possible to definitively identify the nature of the sinks for NO_3 and N_2O_5 within the surface and boundary layers. There are several possibilities, including surface deposition, reaction with NO, reaction of NO_3 with surface-emitted VOC, or an increase in the rate of N_2O_5 hydrolysis near the surface.

Deposition of NO_3 and N_2O_5 would have been most important within the surface layer because of its shallow mixing depth. Assuming a moderately large deposition velocity for NO_3 and/or N_2O_5 of $V_d \sim 1\,cm\,s^{-1}$, their lifetime with respect to deposition, τ_d, within a surface layer of height, h=10–20 m may be estimated as $\tau_d \sim h V_d^{-1}$=15–30 min (Wesely and Hicks, 2000). To our knowledge, deposition velocities for NO_3 and N_2O_5 have not been measured, and deposition losses of these compounds have typically been considered small in comparison to other losses (see, for example, Aldener et al., 2006; Stutz et al., 2004). However, the presence of a shallow surface layer could magnify the importance of deposition. Certainly, vertical gradients in O_3 arising from dry deposition (e.g., Galbally and Roy, 1980) serve to reduce the production rate for NO_3 and N_2O_5 from Reaction (2) as a function of height near the ground surface.

Reaction of NO_3 with NO is often considered to be a more important loss process than deposition near the ground at night because of the emission of NO from either soils or combustion sources and the large rate coefficient for this reaction.

$$NO + NO_3 \rightarrow 2NO_2 \qquad k_7(286\,K) = 2.7 \times 10^{-11}\,cm^3\,s^{-1} \tag{6}$$

In combination with Reaction (2), Reaction (6) leads only to a net increase in the rate

of NO oxidation by O_3 (Reaction 3) and does not lead to a net loss of nitrogen oxides as do NO_3-VOC reactions or N_2O_5 hydrolysis. Therefore, surface NO emissions decrease the impact of NO_3 and N_2O_5 reactions in nocturnal NO_x destruction. At the BAO site, NO may have come from either soil emission or anthropogenic sources. The flux of NO from grassland in autumn in Colorado has been measured in the range 0.2–1 ng N m^{-2} s^{-1} (Williams et al., 1987). The resulting calculated emission rate into a 20 m surface layer is 0.02–0.1 pptv NO s^{-1}, insufficient to titrate a significant amount of ozone. At a constant, 20 ppbv of O_3, the steady state NO concentration resulting from soil emission would have been 3–15 pptv, which would limit the lifetime of NO_3 to 2–10 min. Emission of NO from nearby anthropogenic sources is likely a far larger NO_x source than are soils at this site, as evident from calculated NO_2 concentrations reaching several tens of ppbv. These anthropogenic NO emissions may also have limited the lifetime of NO_3 at the BAO site if the transport time from these sources was short enough that NO was not fully oxidized to NO_2, or if the NO emission was large enough to chemically titrate all of the O_3. For example, the presence of NO may explain the zero NO_3 and N_2O_5 concentrations below 30 m in Fig. 8, where the O_3 mixing ratio was also near zero.

Like NO emission, surface emissions of reactive VOC that are trapped in the surface and/or nocturnal boundary layers may give rise to a rapid NO_3 loss. In contrast to reaction with NO, however, NO_3 reaction with VOC can lead to a net loss of ozone and/or NO_x depending on the VOC (Atkinson and Arey, 2003). In the absence of VOC measurements, however, an estimate of their contribution to NO_3 loss within the boundary layer at the BAO site is difficult. Emission of VOC from grassland consists largely of oxygenated VOC that are not reactive toward NO_3 and are likely not significant at night (Kirstine et al., 1998). Anthropogenic VOC in general are not particularly reactive with NO_3, except for specific classes of less-abundant compounds such as higher alkenes (Wayne et al., 1991).

Hydrolysis of N_2O_5 is a key reaction in the conversion of NO_x to nitric acid or aerosol

nitrate at night.

$$N_2O_5 + H_2O(het) \rightarrow 2HNO_3 \quad (7)$$

The reaction is efficient as a heterogeneous process on aerosol particles. As with NO and VOC, aerosol particle loading (and thus available surface area) is conceivably larger in the NBL than aloft due to trapping of aerosol or aerosol precursor (e.g. ammonia) emissions. Gradients in relative humidity with height above ground may also play a role. Relative humidity at 200 m on 4–5 October ranged between 35–65%, while at 10 m it varied from 60–90%, with an average gradient between these heights of 29% during darkness (see Fig. 3). Therefore, hygroscopic particle growth and/or variation in the uptake coefficient for N_2O_5 with relative humidity could plausibly increase its loss rate to heterogeneous hydrolysis at lower elevations within the NBL.

The preceding discussion demonstrates that the observed variability in NO_3 and N_2O_5 over short distance scales may result from the interaction between the nocturnal stratification of the atmosphere and the distributions of an array of potential NO_3 and N_2O_5 sinks. Furthermore, the reactivity of a compound should be directly related to it variability on both spatial and temporal scales (Junge, 1974). Previous measurements of NO_3 and N_2O_5 at a nearby measurement site (Brown et al., 2003b) showed rapid temporal variation that may have been related to the kind of spatial variability seen in this study. Such small scale variability in sinks is interesting not only from a measurement perspective; it also presents a modeling challenge. The large variability in nitrogen oxide chemistry over small scales means that an accurate representation requires calculation on extremely fine spatial scale or an accurate parameterization of the integration of small scale variations into larger scale models (Jones et al., 2005; Ravishankara, 2005).

The contrast between nitrogen oxide chemistry in the NBL and residual layers underlines the need for more complete vertical profiling studies involving a larger array of chemical and meteorological measurements. This study has primarily illustrated the potential for in-situ chemical measurements from a movable carriage on a tall tower to address this problem. Further measurements at the BAO site that include a larger

array of chemical, aerosol and meteorological instrumentation carried out over longer periods in different seasons, will be of considerable interest.

Acknowledgements. The authors thank W. C. Kuster for the loan of an O_3 monitor. This work was funded by NOAA's Air Quality and Climate Forcing Programs.

References

Aldener, M., et al., Reactivity and loss mechanisms of NO_3 and N_2O_5 in a marin environment: results from in-situ measurements during NEAQS 2002, J. Geophys. Res., in press, 2006.

Aliwell, S. R. and R. L. Jones: Measurements of tropospheric NO_3 at midlatitude, J. Geophys. Res., 103, 5719–5727, 1998.

Allan, B. J., Plane, J. M. C., Coe, H., et al., Observations of NO_3 concentration profiles in the troposphere, J. Geophys. Res., 107, 4588, doi:10.1029/2002JD002112, 2002.

Atkinson, R. and Arey, J.: Atmospheric Degradation of Volatile Organic Compounds, Chem. Rev., 103, 4605–4638, 2003.

Brown, S. S., Neumann, J. A., Ryerson, T. B., et al., Nocturnal odd-oxygen budget and its implications for ozone loss in the lower troposphere. Geophys. Res. Lett. 33, LO8801, doi:8810.1029/2006GL025900, 2006.

Brown, S. S., Stark, H., Ravishankara, A. R., et al.: Applicability of the Steady-State Approximation to the Interpretation of Atmospheric Observations of NO_3 and N_2O_5, J. Geophys. Res., 108, 4539, doi:10.1029/2003JD003407, 2003a.

Brown, S. S., Stark, H., Ryerson, T. B., et al.: Nitrogen oxides in the nocturnal boundary layer: Simultaneous, in-situ detection of NO_3, N_2O_5, NO, NO_2 and O_3, J. Geophys. Res., 108, 4299, doi:10.1029/2002JD002917, 2003b.

Chameides, W. L.: Photo-chemical role of tropospheric nitrogen oxides, Geophys. Res. Lett., 5, 17–20, 1978.

Coe, H., Allan, B. J., Plane, J. M. C., et al.: Retrieval of vertical profiles of NO_3 from zenith sky measurements using an optimal estimation method, J. Geophys. Res., 107, 4587, doi:10.1029/2002JD002111, 2002.

Dubé, W. P., Brown, S. S., Osthoff, H. D., et al., Aircraft instrument for simultaneous, in-situ measurements of NO_3 and N_2O_5 via cavity ring-down spectroscopy, Rev. Sci. Instr., 77, 034101, 2006.

Fish, D. J., Shallcross, D. E., Jones, R. L., et al., The vertical distribution of NO_3 in the atmospheric boundary layer, Atmos. Environ., 33, 687–691, 1999.
Galbally, I. E. and C. R. Roy: Destruction of ozone at the earth's surface, Quart. J. R. Met. Soc., 106, 599–620, 1980.
Galmarini, S., Duynkerke, P. G., deArellano, I. V. G., et al.: Evolution of nitrogen oxide chemistry in the nocturnal boundary layer, J. Appl. Meteor., 36, 943–957, 1997.
Geyer, A. and Stutz, J.: Vertical profiles of NO_3, N_2O_5, O_3, and NO_x in the nocturnal boundary layer: 2. Model studies on the altitude dependence of composition and chemistry, J. Geophys. Res., 109, D12307, doi:10.1029/2003JD004211, 2004a.
Geyer, A. and Stutz, J.: The vertical structure of OH-HO[2]-RO[2] chemistry in the nocturnal boundary layer: A one-dimensional model study, J. Geophys. Res., 109, D16301, doi:10.1029/2003JD004425, 2004b.
Hahn, C. J.: A Study Of The Diurnal Behavior Of Boundary-Layer Winds At The Boulder Atmospheric Observatory, Boundary-Layer Meteorology, 21, 231–245, 1981.
Heintz, F., Platt, U., Flentje, J., et al.: Long-term observation of nitrate radicals at the Tor Station, Kap Arkona (Rügen), J. Geophys. Res., 101, 22 891–22 910, 1996.
Jones, R. L., Ball, S. M., Shallcross, D. E., et al.: Small scale structure in the atmosphere: implications for chemical composition and observational methods, Faraday Discuss., 130, 165–179, 2005.
Junge, C. E.: Residence time and variability of tropospheric trace gases, Tellus, 26, 477–488, 1974.
Kaimal, J. C. and J. E.: Gaynor, The Boulder Atmospheric Observatory, J. Climate Appl. Meteorol., 22, 863–880, 1983.
Kirstine, W., Galbally, I., Ye, Y., et al.: Emissions of volatile organic compounds (primarily oxygenated species) from pasture, J. Geophys. Res., 103, 10 605–10 619, 1998.
Platt, U. F., Winer, A. M., Bierman, H. W., et al.: Measurement of Nitrate Radical Concentrations in Continental Air, Environ. Sci. Technol., 18, 365–369, 1984.
Povey, I. M., South, A. M., de Roodenbeke, A. T. K., et al.: A broadband lidar for the measurement of tropospheric constituent profiles from the ground, J. Geophys. Res., 103, 3369–3380, 1998.
Ravishankara, A. R.: Chemistry-climate coupling: the importance of chemistry in climate issues, Faraday Discuss., 130, 9–26, 2005.
Richards, L. W.: Comments on the oxidation of NO2 to nitrate – Day and night, Atmos. Environ.,

17, 397–402, 1983.
Riemer, N., Vogel, H., Vogel, B., et al.: Impact of the heterogeneous hydrolysis of N_2O_5 on chemistry and nitrate aerosol formation in the lower troposphere under photosmog conditions, J. Geophys. Res., 108, 4144, doi:10.1029/2002JD002436, 2003.
Saiz-Lopez, A., Shillito, J. A., Coe, H., et al.: Measurements and modelling of I2, IO, OIO, BrO and NO3 in the mid-latitude marine boundary layer, Atmos. Chem. Phys., 6, 1513–1528, 2006.
Sander, S. P., Friedl, R. R., Golden, D. M., et al.: Chemical Kinetics and Photochemical Data for Use in Atmospheric Studies, JPL Publication 02-25, Pasadena, CA, 2003.
Smith, J. P. and Solomon, S.: Atmospheric NO3 3. Sunrise Disappearance and the Stratospheric Profile, J. Geophys. Res., 95, 13 819–13 827, 1990.
Smith, J. P., Solomon, S., Sanders, R. W., et al.: Atmospheric NO3 4. Vertical Profiles at Middle and Polar Latitudes at Sunrise, J. Geophys. Res., 98, 8983–8989, 1993.
Stull, R. B.: An Introduction to Boundary Layer Meteorology, Kluwer Academic, Dordrecht, The Netherlands, 1988.
Stutz, J., Alicke, B., Ackermann, R., et al.: Vertical profiles of NO_3, N_2O_2, O_3, and NO_x in the nocturnal boundary layer: 1. Observations during the Texas Air Quality Study 2000, J. Geophys. Res., 109, D12306, doi:10.1029/2003JD004209, 2004.
Vanvalin, C. C. and E. Ganor: Air-Pollution Measurements At The Boulder-Atmospheric-Observatory, Water Air And Soil Pollution, 35, 357–372, 1987.
von Friedeburg, C., Wagner, T., Geyer, A., et al.: Derivation of tropospheric NO_3 profiles using off-axis differential optical absorption spectroscopy measurements during sunrise and comparison with simulations, J. Geophys. Res.-Atmos., 107, 4168, doi:10.1029/2001JD000481, 2002.
Wang, S., Ackermann, R., Stutz, J., et al.: Vertical profiles of NOx chemistry in the polluted nocturnal boundary layer in Phoenix, AZ: I. Field observations by long-path DOAS, Atmos. Chem. Phys., 6, 2671–2693, 2006.
Wayne, R. P., Barnes, I., Biggs, P., et al.: The Nitrate Radical: Physics, Chemistry, and the Atmosphere, Atmospheric Environment Part A — General Topics, 25, 1–203, 1991.
Weaver, A., Solomon, S., Sanders, R. W., et al.: Atmospheric NO3 5. Off-axis measurements at sunrise: Estimates of tropospheric NO3 at 40° N, J. Geophys. Res., 101, 18 605–18 612, 1996.
Wesely, M. L. and Hicks, B. B.: A review of the current status of knowledge on dry deposition,

Atmos. Environ., 34, 2261–2282, 2000.
Williams, E. J., Parrish, D. D., Fehsenfeld, F. C., et al.: Determination of Nitrogen Oxide Emissions From Soils: Results from a Grassland Site in Colorado, United States, J. Geophys. Res., 92, 2173–2179, 1987.

Fig. 1. Map of the Denver-Boulder area (Colorado, USA) showing the location of the Boulder Atmospheric Observatory (BAO).

ACPD
6, 9431–9458, 2006

EGU

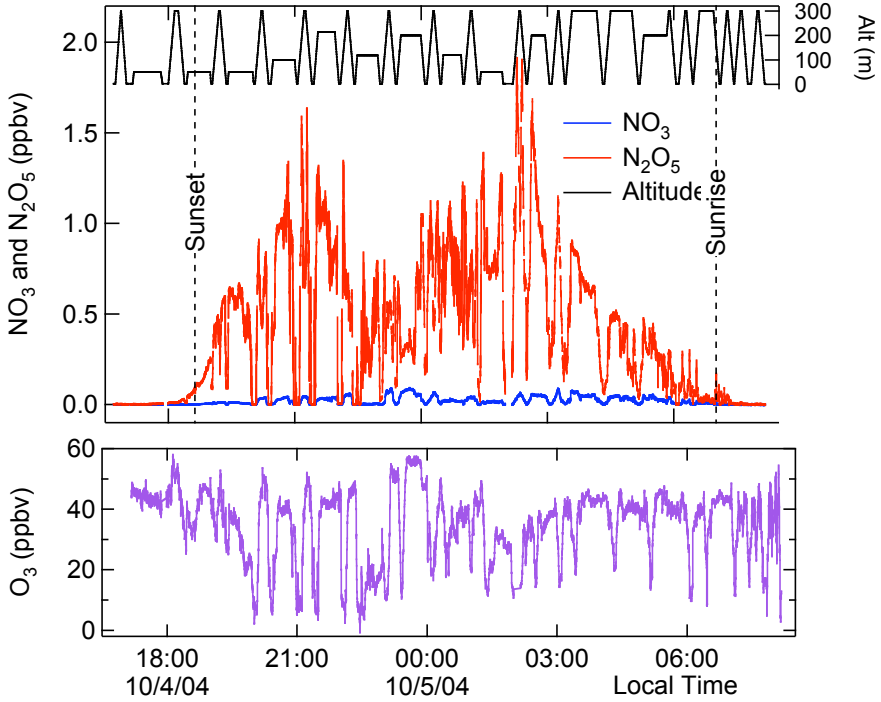

Fig. 2. Time series of the measured mixing ratios of NO_3, N_2O_5 (top graph) and ozone (bottom graph). The altitude derived from the pressure measurements appears above the top graph against the right axis.

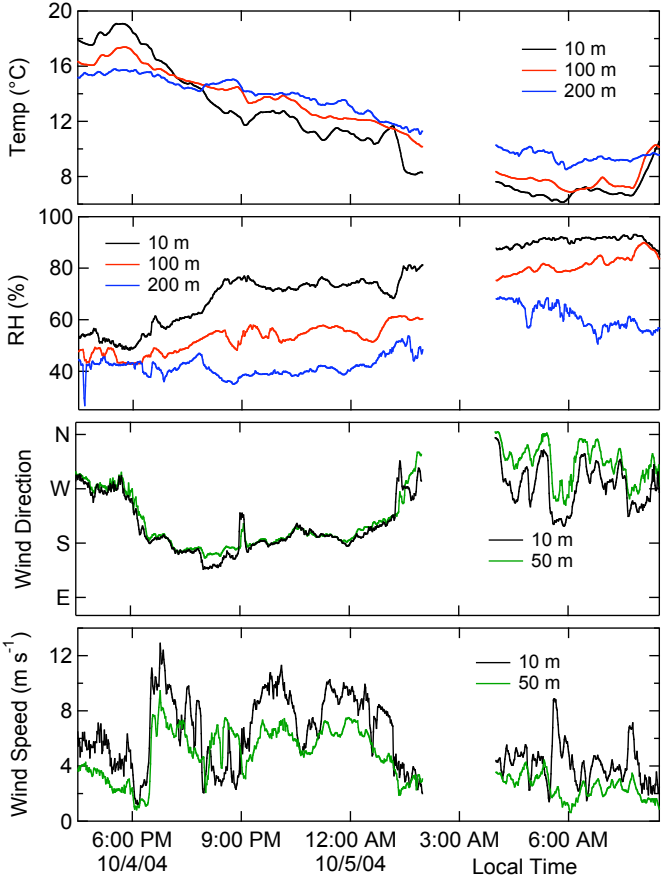

Fig. 3. Time series of meteorological data at fixed heights on the tower. Temperature and relative humidity were available from 10, 100 and 200 m, while wind direction and speed were available from 10 and 50 m only.

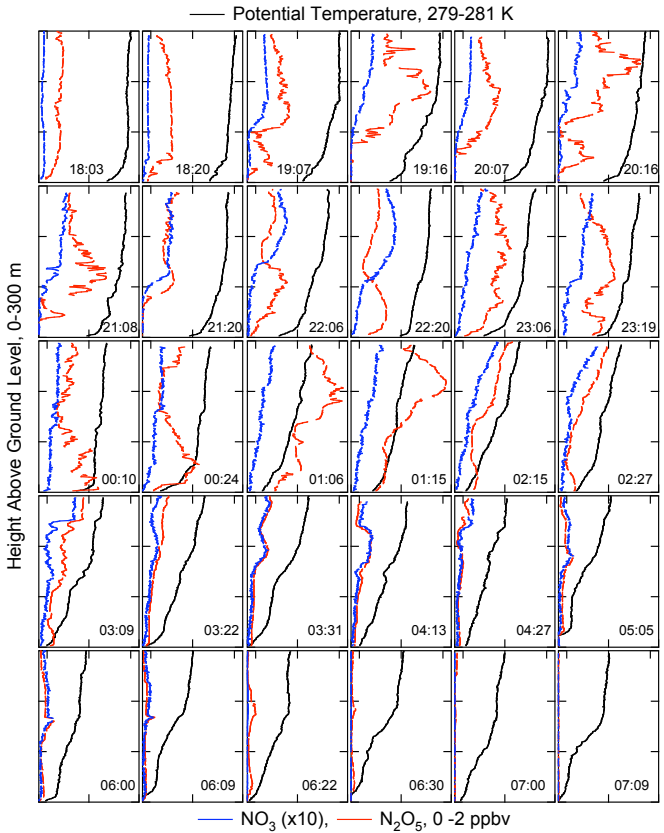

Fig. 4. Overview of 30 profiles from just prior to sunset to just after sunrise on 4–5 October. NO_3 (blue, multiplied by 10) and N_2O_5 (red) are shown against the bottom axis of each plot against a uniform scale from 0–2 ppbv. Potential temperature (black) is shown against the top axis of each plot on a uniform scale from 279–291 K. The left axes are altitude from 0–300 m. The time on each plot corresponds to the approximate midpoint of the profile.

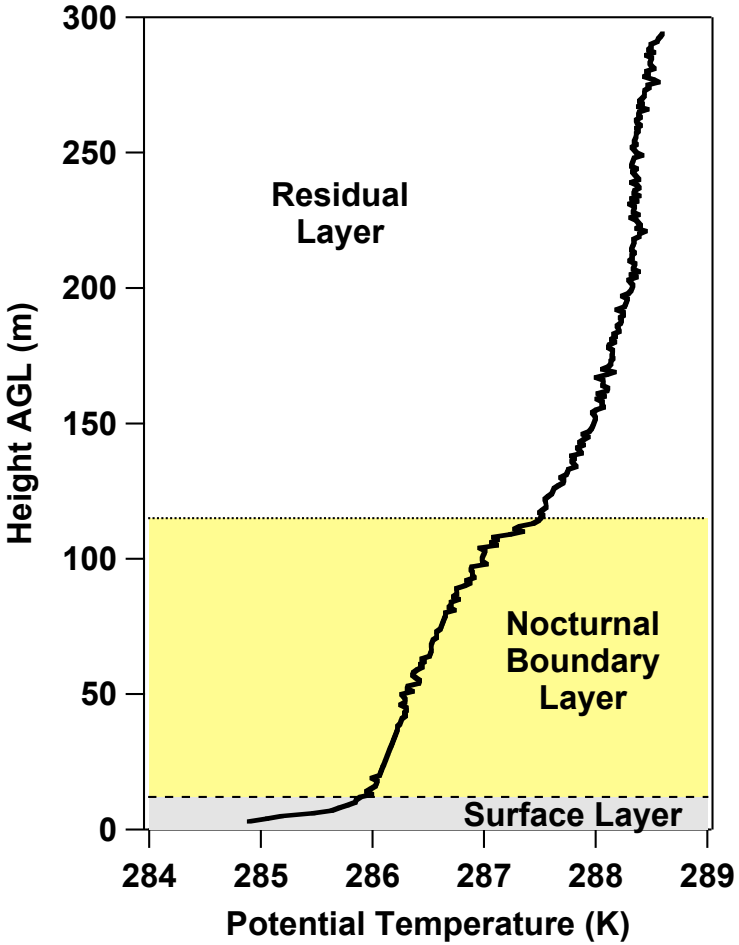

Fig. 5. Representative nocturnal potential temperature profile with labels for the most commonly observed layers, as described in the text.

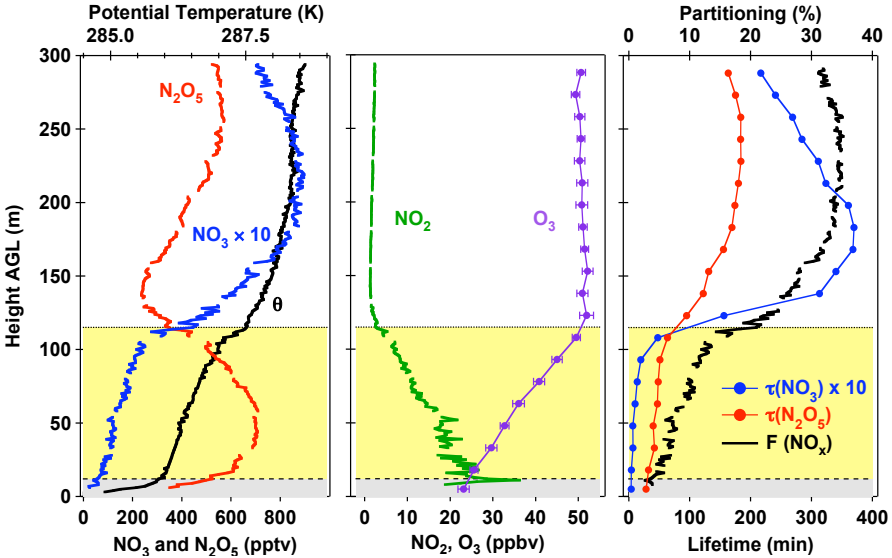

Fig. 6. Left: Profile of NO_3 and N_2O_5 (bottom axis), and potential temperature (top axis) as a function of height above ground level (AGL) from 22:16–22:24 on 4 October 2004. Note that the NO_3 mixing ratio has been multiplied by a factor of 10 to display it on the same scale with N_2O_5. Center: Vertical profiles of O_3 (measured at 18 s time resolution) and NO_2, calculated from the measured NO_3, N_2O_5 and temperature according to Eq. (1). Right: Profile of NO_3 and N_2O_5 lifetimes (bottom axis) calculated according to Eq. (4) (with $\tau(NO_3)$ multiplied by 10) and partitioning, $F(NO_x)$ (top axis) from Eq. (5). The horizontal lines and color coding indicate the layer assignments according to the scheme shown in Fig. 5.

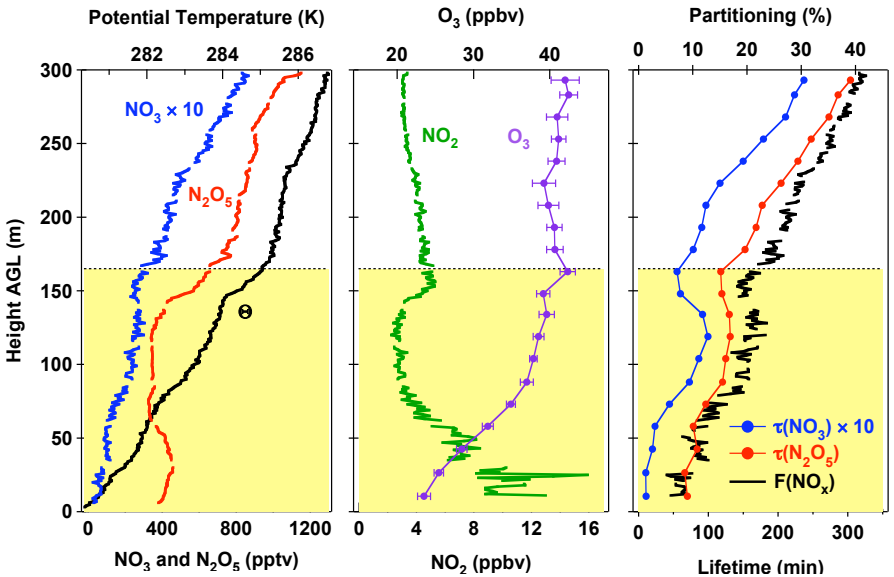

Fig. 7. Same as Fig. 6, except for a profile from 02:11–02:20. Note that O_3 is displayed against the top axis in the center graph in this figure. The layering color scheme is the same as for Fig. 5, except that the surface layer is absent.

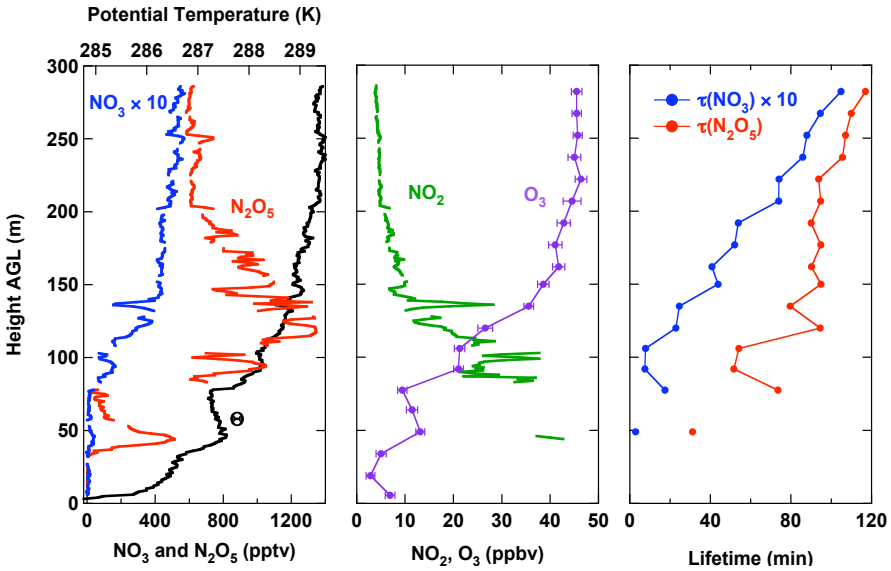

Fig. 8. Same as Fig. 6, except for a profile from 21:04–21:13.

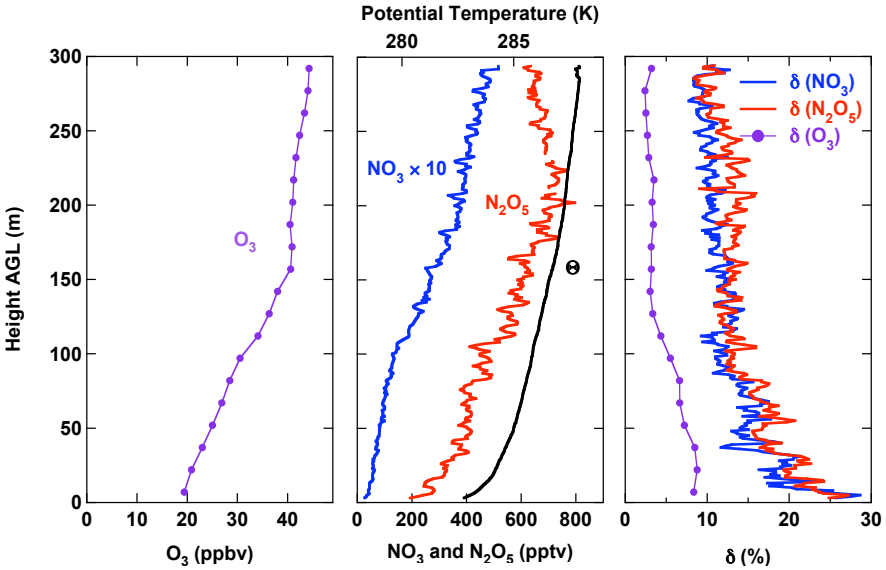

Fig. 9. Vertical profiles of averaged O_3 (left graph) NO_3, N_2O_5 and potential temperature (Θ) (right graph) for 27 profiles between 4 October 2004 19:00–5 October 2004 06:00. The relative standard deviation of NO_3, N_2O_5 and O_3 (see text) are shown in the right graph. The apparently systematic oscillations in the averages are an artifact of the frequency at which zero measurements were taken during vertical ascents and descents.